IRAQI JOURNAL OF APPLIED PHYSICS
Vol. 22, No. 1, January-March 2026, pp. 91-98

Farid Okbi [1,2*]
Sonia Bouzgarrou [3]
Said Lakel [4]
Mohamed Mahfoud [1]

[1] Department of Science and Technology, Faculty of Applied Sciences, Ibn Khaldoun University, Tiaret, 14000 ALGERIA
[2] Laboratory of Materials for Application and Valorization of Renewable Energy (LMAVER), Amar Telidji University, Laghouat, 03000 ALGERIA
[3] Department of Physics, College of Science, Qassim University, Buraidah, SAUDI ARABIA
[4] Laboratory of Metallic and Semiconducting Materials, University of Biskra, Biskra 07000, ALGERIA
*Corresponding author: farid.okbi@univ-tiaret.dz

Investigation of Pressure Effect on Structural and Optoelectronic Properties of $Al_{0.75}Sc_{0.25}P$ Structure Using Density Functional Theory

The structural, electronic, and optical properties of AlP and $Al_{0.75}Sc_{0.25}P$ were investigated through a series of under hydrostatic pressures from 0 to 15 GPa using Density Functional Theory (DFT) with the PBE-GGA functional. This pressure range was chosen to retain the zinc-blende structure and avoid phase transition. The lattice constant for $Al_{0.75}Sc_{0.25}P$ decreased from 5.620 Å to 5.350 Å. The direct band gap decreased slightly from 1.833 eV to 1.814 eV. Conversely, the indirect band gap increased from 2.52 eV to 2.67 eV. The optical properties demonstrated nonlinear dependence on pressure; the static dielectric constant and refractive index both decreased before increasing. The Sc concentration (x = 0.25) was chosen to enhance properties without significant structural distortion. Despite experimental challenges, including AlP instability in humid conditions and high-pressure limitations, this study provides valuable insights into the pressure-tunable behavior of AlP-based materials for potential optoelectronic applications.

Keywords: Density functional theory; Optical properties; Electronic properties; Optoelectronics
Received: 10 April 2025; Revised: 26 July 2025; Accepted: 2 August 2025; Published: 1 January 2026

1. Introduction

Aluminum phosphide (AlP) is an indirect band gap semiconductor with a band gap of approximately 2.5 eV [1], which makes it a promising candidate for various optoelectronic applications, including infrared photodetectors and high-temperature electronic devices. Under standard conditions, AlP adopts the zinc-blende (ZB) crystal structure (space group F-43m) [2,3]. However, it exhibits a strong pressure dependence, undergoing phase transitions to more compact structures such as NiAs, Cmcm, and CsCl under high-pressure conditions [4,5], which significantly affect its electronic and structural characteristics. Furthermore, the experimental investigation of AlP is hindered by its instability in humid environments, emphasizing the need for theoretical approaches.

To overcome these limitations and enable property engineering, alloying AlP with compatible compounds such as scandium phosphide (ScP) has emerged as a viable strategy. Both AlP and ScP crystallize in the ZB structure and exhibit full miscibility, enabling the formation of stable $Al_{1-x}Sc_xP$ alloys over the entire composition range without phase segregation [6]. In particular, doping AlP with scandium (Sc) allows for controlled tuning of the band gap within the 2.0-2.5 eV range, offering enhanced versatility across optical and infrared optoelectronic applications.

Despite this potential, most existing theoretical studies on $Al_{1-x}Sc_xP$ have been restricted to ambient pressure conditions. However, in real-world environments, devices are often subject to external mechanical stresses, necessitating a deeper understanding of pressure-dependent behavior. While some studies have explored pressure effects in related III-V compounds, systematic investigations of $Al_{1-x}Sc_xP$ alloys under hydrostatic pressure remain scarce.

This study addresses this gap by examining the influence of hydrostatic pressure (0-15 GPa) on the structural, electronic, and optical properties of the $Al_{0.75}Sc_{0.25}P$ ternary alloy, along with its binary counterpart AlP. Using density functional theory (DFT) within the plane-wave pseudopotential framework as implemented in the CASTEP code [7,8], we aim to provide critical insights into the pressure-induced modifications in these materials. Our findings contribute to the rational design of AlP-based semiconductors for robust and efficient performance in advanced optoelectronic devices operating under varying environmental conditions.

2. Method of Calculations

In this study, we employed the CASTEP code to perform calculations using the plane-wave pseudo potential method within the framework of density functional theory (DFT) [9, 10]. The generalized gradient approximation (GGA) with the Perdew-

 © ALL RIGHTS RESERVED

Burke-Ernzerhof (PBE) [11] was applied for the exchange-correlation function. We focused on examining the effects of pressure on various parameters, including lattice constants, band gap energies, and optical properties. To investigate the structural, electronic, and optical properties of $Al_{0.75}Sc_{0.25}P$ under pressure, we utilized a 1×1×1 super cell for AlP, where one Al atom was replaced by an Sc atom. The number of conduction bands is another key parameter, as it defines the energy range and plays a crucial role in determining the accuracy of the Kramers-Kronig transformation. The interaction between ions and electrons was described using the OTFG ultra soft pseudo potential [12]. The kinetic energy cutoff for plane waves was set to ultrafine, and an ultrafine k-point mesh, based on the Monkhorst-Pack scheme [13, 14], was employed for the super cell system. Geometry optimization was performed using the minimization technique of the Broyden-Fletcher-Goldfarb-Shanno (BFGS) algorithm [15,16].

Additionally, we investigated the structural, electronic, and optical properties of $Al_{0.75}Sc_{0.25}P$ ternary alloys, along with their ordered AlP and ScP binary counterparts, under hydrostatic pressure ranging from 0 to 15 GPa.

3. Results and Discussion

3.1 Structural Properties Under Pressure

We computed the structural properties of binary AlP, and the ternary $Al_{0.75}Sc_{0.25}P$ alloy in the zinc-blende structure. The results for the lattice constants and bulk modulus at 0, 5, 10, and 15 GPa are listed in table (1). To evaluate the quality of our results, we compared them with values obtained from other theoretical methods and experimental data, and we found that our results were in good agreement with the available experimental and theoretical values [17-23]. The variation of the lattice constant as a function of pressure for the ternary $Al_{0.75}Sc_{0.25}P$ alloy in the pressure range of 0 to 15 GPa is presented in Fig. (1).

At zero pressure, the lattice constant is a = 5.620Å. We chose a pressure range below the transition pressure to avoid possible phase transitions. As pressure increases, the lattice constant decreases, which is consistent with the general behavior of materials under pressure. This decrease in the lattice constant with increasing pressure is due to the strengthening of atomic repulsion, leading to a reduction in both the lattice parameters and the overall volume. The introduction of Scandium (Sc) atoms into the AlP lattice has a noticeable impact on the structural properties, particularly under pressure. The larger atomic radius of scandium compared to aluminum causes an expansion of the lattice at low pressures. However, as pressure increases, the scandium atoms exert a greater influence on the lattice contraction due to their larger atomic size and the stronger repulsive forces between atoms. This effect results in a more significant increase in the lattice constant for the $Al_{0.75}Sc_{0.25}P$ alloy compared to pure AlP, the scandium atoms help stabilize the material, enhancing the overall structural integrity of the alloy.

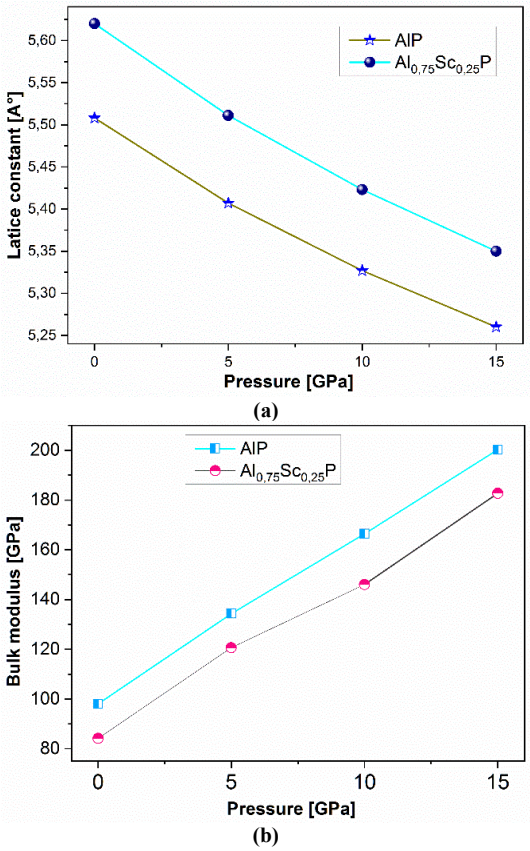

Fig. (1) Variations of (a) the lattice constant and (b) bulk modulus as functions of pressure for $Al_{0.75}Sc_{0.25}P$ ternary alloy

3.2 Pressure Effect on Band Gap and Density of States

To investigate the effects of hydrostatic pressure on the energy band gap, we examined the band energies at selected symmetry points under hydrostatic pressure in the range of 0 to 15 GPa. The results of band structure of $Al_{0.75}Sc_{0.25}P$ are shown in Fig. (3), that at 0, 5, 10, and 15 GPa, the maximum of the valence band is located at the G point, while the conduction band minimum is also located at the G point, indicating that the compound exhibits a direct band gap across these pressure values. The variation of the direct and indirect band gap for AlP and $Al_{0.75}Sc_{0.25}P$ alloy as a function of hydrostatic pressure from 0 to 15 GPa is shown in Fig. (2). It is evident that the band gap remains direct with increasing pressure for the $Al_{0.75}Sc_{0.25}P$ compound at 0, 5, 10, and 15 GPa. Moreover, figure (2) demonstrates that the direct band gap of both compounds increases with increasing pressure, whereas the indirect band gap decreases as the pressure increases.

 © ALL RIGHTS RESERVED

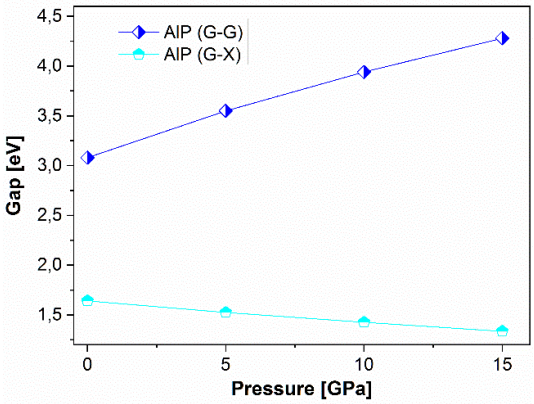

(a)

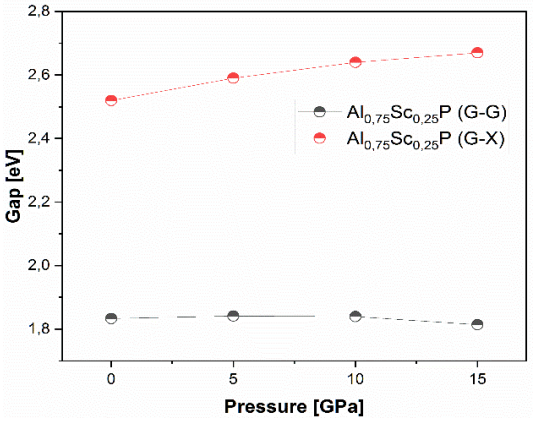

(b)

Fig. (2) Changes in the band gap energy of (a) AlP and (b) ternary $Al_{0.75}Sc_{0.25}P$ alloy with different pressures

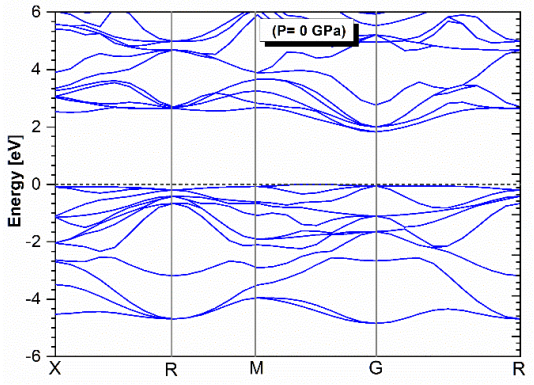

(a)

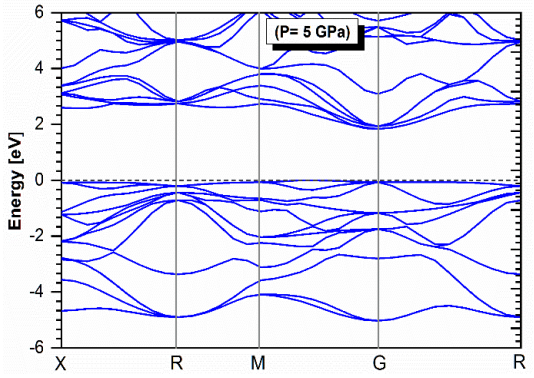

(b)

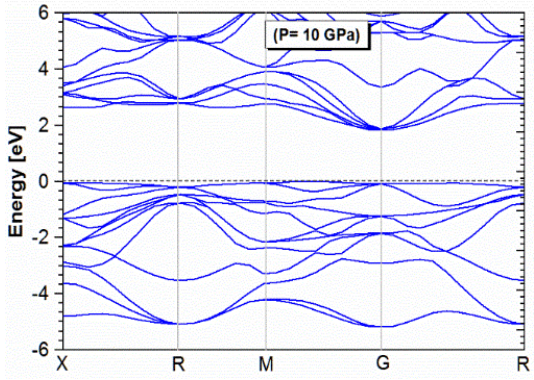

(c)

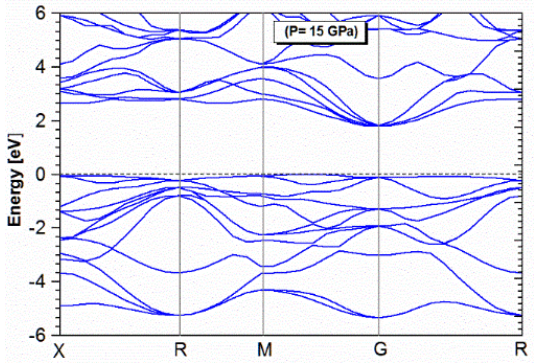

(d)

Fig. (3) Calculated band structure of $Al_{0.75}Sc_{0.25}P$ at ((a) 0; (b) 5; (c) 10 and (d) 15 Gpa)

For AlP, the compound maintains an indirect band gap throughout the entire applied pressure range, as shown in Fig. (2a). On the other hand $Al_{0.75}Sc_{0.25}P$ semiconductors exhibit direct band gaps throughout the entire pressure range, as seen in Fig. (2b). under stress-free conditions, the band gap of the ternary $Al_{0.75}Sc_{0.25}P$ alloy is 1.833 eV. It is evident from Fig. (2b) that the $Al_{0.75}Sc_{0.25}P$ alloy remains a direct band-gap semiconductor in the pressure range of 0 to 15 GPa. Moreover, as pressure increases, the band gap shrinks. The relationship between the band gap and pressure can be expressed by the following equation:

$$E_g(P) = E_g(0) + \alpha P + \beta P^2 \qquad (1)$$

where α and β are the pressure coefficients

For AlP, the calculated band gap is 1.641 eV, which is smaller than the experimental value of 2.5 eV [25], but closer to values of 1.54 eV [26] and 1.49 eV [27] reported in the literature. This discrepancy is mainly due to the underestimation of the electronic exchange interactions when using the GGA approximation. Despite this, the lower calculated value does not affect the analysis of the electronic structure in this study. The results for the direct and indirect energy gaps of the binary compounds AlP, and the ternary alloy $Al_{0.75}Sc_{0.25}P$ are given in table (2).

The partial density of states (PDOS) for $Al_{0.75}Sc_{0.25}P$ at 0, 5, 10, and 15 GPa is shown in Fig. (4). Figure. (4a) illustrates the density of states (DOS) for the $Al_{0.75}Sc_{0.25}P$ compound at 0 GPa. The top magenta

 © ALL RIGHTS RESERVED

curve represents the total DOS, reflecting the electronic states available per unit energy (states/eV) across the energy range. The Fermi level (at E=0) marks the boundary between occupied and unoccupied states. For the contributions from atomic orbitals, the P 3p and P 3s orbitals show significant contributions near the valence band maximum (below E=0), highlighting the importance of phosphorus in bonding. The Sc 3d, Sc 3p, and Sc 4s orbitals exhibit noticeable contributions in the conduction band (above E=0), indicating their role in conduction properties. Meanwhile, the Al 3p and Al 3s orbitals mainly contribute to the valence band and participate in hybridization with phosphorus. The figure covers a wide energy range from -30 eV to 17 eV, emphasizing both deep-lying core states and the edges of the valence and conduction bands. As hydrostatic pressure increases, significant changes occur in the projected density of states due to altered atomic interactions and lattice compression. Pressure leads to enhanced hybridization between Sc and Al orbitals with P orbitals, shifting the peak positions in the projected DOS closer to the energy levels at the edges of the valence and conduction bands. The separation between the peaks of the valence and conduction bands in the projected density of states increases, corresponding to an expanded direct band gap under higher pressure. Pressure also concentrates states near the conduction band edge, especially in Sc 3d and P 3p orbitals, enhancing their contribution to conduction. A shift in the energy positions of certain orbitals, such as Sc 3d and Al 3p, occurs under pressure, leading to a redistribution of states within the valence and conduction bands.

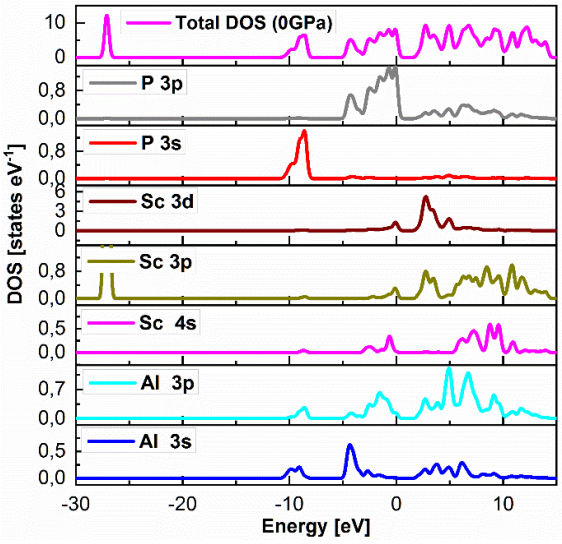

(a)

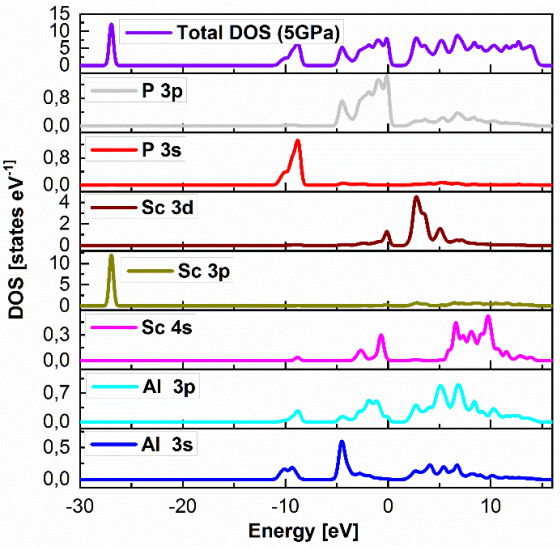

(b)

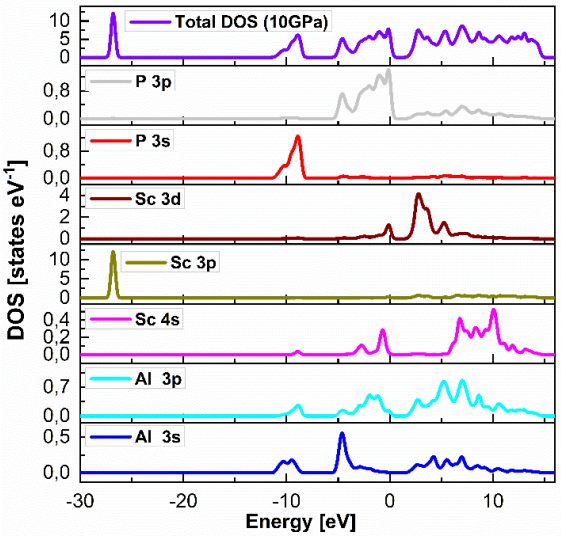

(c)

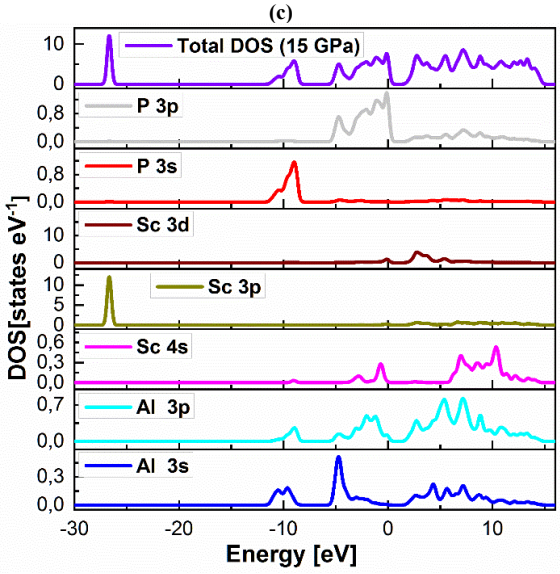

(d)

Fig. (4) Total and Partial Density of States (DOS, PDOS) for $Al_{0.75}Sc_{0.25}P$ at different pressures ((a) 0; (b) 5; (c) 10 and (d) 15 Gpa)

 © ALL RIGHTS RESERVED

Hydrostatic pressure plays a crucial role in modifying the electronic properties of the $Al_{0.75}Sc_{0.25}P$ compound by affecting hybridization, peak positions, and the band gap. These changes reflect the compound's response to pressure, making it a promising candidate for electronic applications under varying pressure conditions.

3.3 Pressure Effect on the Optical Properties

In this section, we calculate the optical properties of the ternary $Al_{0.75}Sc_{0.25}P$ alloy under different pressure values (0 GPa, 5 GPa, 10 GPa, and 15 GPa), which are crucial for their applications. The optical properties can be derived from the complex dielectric function ε(ω), given by the following relation:

$$\varepsilon(\omega) = \varepsilon_1(\omega) + i\,\varepsilon_2(\omega) \quad (2)$$

where $\varepsilon_1(\omega)$ and $\varepsilon_2(\omega)$are the real and imaginary parts of the complex dielectric function, respectively.

Figure (5) presents the imaginary parts $\varepsilon_2(\omega)$ and the real parts $\varepsilon_1(\omega)$ of the dielectric function, while figures (6) and (7) represent the optical constants (refractive index n(ω), extinction coefficient k(ω), and absorption coefficient) of $Al_{0.75}Sc_{0.25}P$ at different pressures (0, 5, 10 and 15 GPa). These constants are calculated from the real and imaginary parts of the dielectric function. The relevant equations for these properties are as follows [1]:

$$n(\omega) = \frac{\left[\sqrt{\varepsilon_1(\omega)^2+\varepsilon_2(\omega)^2}+\varepsilon_1(\omega)\right]^{1/2}}{\sqrt{2}} \quad (3)$$

$$\alpha(\omega) = \frac{2\sqrt{2}\pi\left[\sqrt{\varepsilon_1(\omega)^2+\varepsilon_2(\omega)^2}-\varepsilon_1(\omega)\right]^{1/2}}{\lambda} \quad (4)$$

$$k(\omega) = \frac{\left[\sqrt{\varepsilon_1(\omega)^2+\varepsilon_2(\omega)^2}-\varepsilon_1(\omega)\right]^{1/2}}{\sqrt{2}} \quad (5)$$

$$L(\omega) = Im\left(\frac{-1}{\varepsilon(\omega)}\right) = \frac{\varepsilon_2(\omega)}{[\varepsilon_1^2(\omega)+\varepsilon_2^2(\omega)]} \quad (6)$$

It is important to note that the spectra under the influence of pressure shift towards higher energy values, accompanied by a slight increase in their amplitudes.

As pressure is applied, the curves for the real parts of the dielectric function coincide, remaining almost identical. The application of high pressure pushes the valence band towards lower energies, while the conduction band minimum shifts towards higher energies. This leads to a change in the gap energy due to the transition, as well as an increase in the band gap. As a result, there is a change in the optical transition between the maximum of the valence band and the minimum of the conduction band.

The dielectric constant $\varepsilon_1(0)$ and refractive index n(0) results are provided in Table (3), along with previously reported theoretical data. It is clear that our results are in good agreement with the theoretical values at P = 0 GPa for AlP, and $Al_{0.75}Sc_{0.25}P$, and they are compared with the theoretical values [19,29] as well as the available experimental data [30].

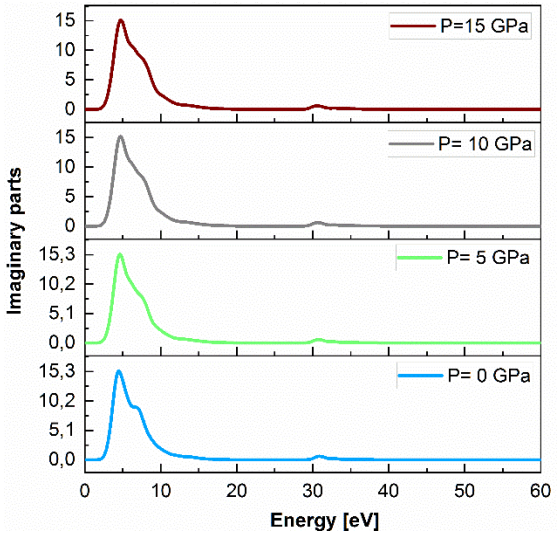

Fig. (5) (a) Imaginary parts $\varepsilon_2(\omega)$ and (b) real parts $\varepsilon_1(\omega)$ of the dielectric function of $Al_{0.75}Sc_{0.25}P$ at different pressures (0, 5, 10 and 15 Gpa)

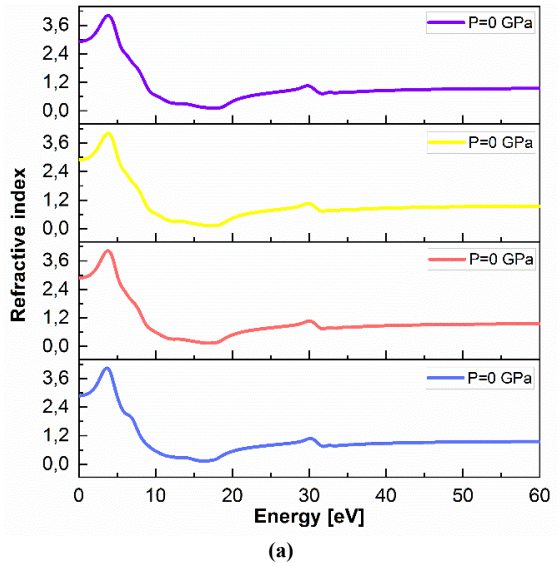

 © ALL RIGHTS RESERVED

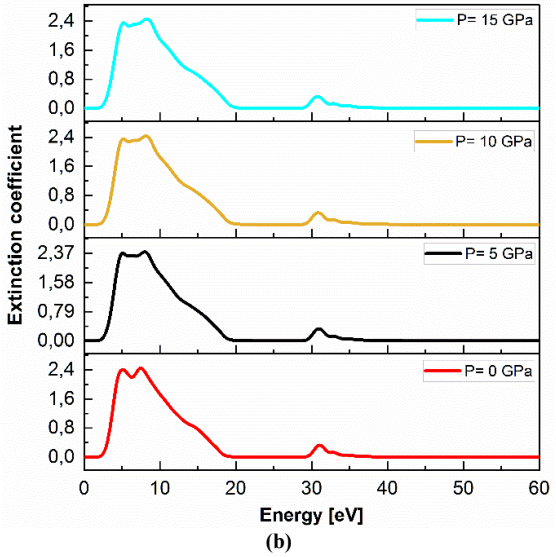

Fig. (6) (a) Refractive index n(ω) and (b) extinction coefficient k(ω) of $Al_{0.75}Sc_{0.25}P$ at different pressures (0, 5, 10 and 15 Gpa)

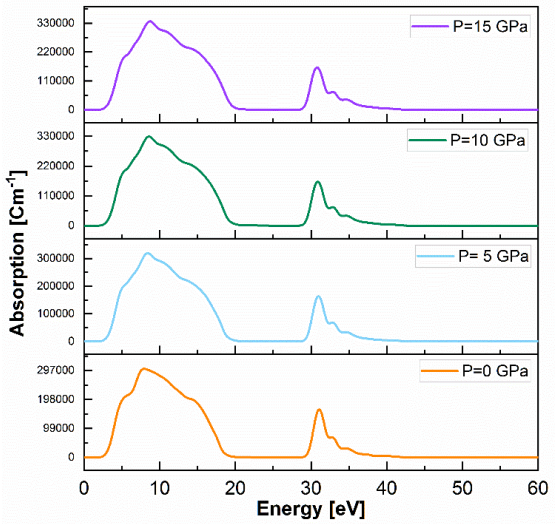

Fig. (7) Absorption coefficient of $Al_{0.75}Sc_{0.25}P$ at different pressures (0, 5, 10 and 15 Gpa)

Additionally, we calculated the absorption coefficient α(ω) at different pressures (0, 5, 10, and 15 Gpa), as shown in Fig. (7). It can be observed that the absorption starts at different energies for each pressure value. These values are derived from our calculations and represent the onset of absorption at the given pressures.

4. Conclusion

This research investigated the structural, electronic, and optical properties of AlP and $Al_{0.75}Sc_{0.25}P$ alloy under hydrostatic pressure using DFT with GGA-PBE level of theory. Optimized parameters such as lattice constants, band structure, and optical functions were computed. The findings demonstrated that pressure can actively alter both the electronic structure and the optical response of the materials investigated. More specifically, with respect to $Al_{0.75}Sc_{0.25}P$, the direct band gap responded to pressure by slightly decreasing, while the indirect band gap increased, showing pressure induced band reordering. Additionally, many of the optical functions, such as absorption spectra and dielectric functions, this work contributes to understanding pressure dependence on III-V semiconductors and demonstrates potential for AlScP alloys to be used in tunable optoelectronic applications.

References

[1] M.P. Thompson et al., "Deposition factors and band gap of zinc-blende AlN", *J. Appl. Phys.*, 89(6) (2001) 3331-3336.

[2] S. Lakel, F. Okbi and H. Meradji, "Optical and electronic properties of BxAl1-xP alloys: A first principles study", *Optik*, 127 (2016) 3755-3761.

[3] M.J. Herrera-Cabrera, P. Rodríguez-Hernández and A. Muñoz, "Theoretical study of the elastic properties of III-P compounds", *phys. stat. sol. (b)*, 223 (2011) 411-415.

[4] B. Ghebouli et al., "First-principles study of structural, elastic, electronic and lattice dynamic properties of $As_xP_yN_{1-x-y}Al$ quaternary alloys", *J. Alloys Compd.*, 507 (2010) 120-125.

[5] P. Friedel, M.S. Hybertsen and M. Schluter, "Local empirical pseudopotential approach to the optical properties of Si/Ge superlattices", *Phys. Rev. B*, 39(11) (1989) 7974-7981.

[6] A. Benamrani, S. Daoud and P.K. Saini, "Structural, elastic and thermodynamic properties of ScP compound: DFT study", *J. Nano-Electron. Phys.*, 13(2) (2021) 02012.

[7] M.D. Segall et al., "First-principles simulation: ideas, illustrations and the CASTEP code", *Phys. Condens. Matter*, 14 (2002) 2717-2744.

[8] M.J. Rutter, "C2x: A tool for Visualization and input preparation for CASTEP and other electronic structure codes", *Comput. Phys. Commun.*, 225 (2018) 174-179.

[9] W. Kohn and L.J. Sham, "Self-consistent equations including exchange and correlation effects", *Phys. Rev.*, 140 (1965) 1133-1138.

[10] D. Bagayoko, "Understanding density functional theory (DFT) and completing it in practice", *AIP Adv.*, 4(12) (2014) 127104.

[11] J.P. Perdew, K. Burke and M. Ernzerhof, "Generalized gradient approximation made simple", *Phys. Rev. Lett.*, 77 (1996) 3865-3868.

[12] N. Troullier and J.L. Martins, "Efficient pseudopotentials for plane-wave calculations", *Phys. Rev. B*, 43 (1991) 1993-2006.

[13] H.J. Monkhorst and J.D. Pack, "Special points for Brillouin-zone integrations", *Phys. Rev. B*, 13 (1976) 5188-5192.

[14] T. Lalmuanchhana et al., "Strain induced modification of CdO monolayer electronic properties", *AIP Conf. Proc.*, 2265(1) (2020) 050002.

 © ALL RIGHTS RESERVED

[15] B.G. Pfrommer et al., "Relaxation of crystals with the quasi-Newton method", *J. Comput. Phys.*, 131 (1997) 233-240.
[16] J. Wu, Y. Huang and V. Nguyen, "On the BFGS monolithic algorithm for the unified phase field damage theory", *Comput. Meth. Appl. Mech. Eng.*, 360 (2020) 112767.
[17] K.H. Hellwege, in **Semiconductors: Intrinsic Properties of Group IV Elements and III-V, II-VI and I-VII Compounds**, Landolt-Börnstein New Series, Group III, vol. 22, O. Madelung (ed.), Springer (Berlin, 1982).
[18] F. Annane, et al., "First-principle investigation of AlAs and AlP compounds and ordered $AlAs_{1-x}P_x$ alloys", *Comput. Mater. Sci.*, 50 (2010) 274.
[19] Z.Y. Jiao et al., "Simulation of optical function for phosphide crystals following the DFT band structure calculations, *Theor. Chem. Acc.*, 970 (2011) 79.
[20] R.W.G. Wyckoff, **"Crystal Structures"**, 2nd ed., Krieger (Malabar, 1986).
[21] F. Okbi et al., "First principles study on electronic structure and optical properties of ternary semiconductor $In_xAl_{1-x}P$ alloys", *Semicond.*, 54 (2020) 58-66.
[22] A. Bouhemadou et al., "FP-APW+lo calculations of the elastic properties in zinc-blende III-P compounds under pressure effects", *Comput. Mater. Sci.*, 45 (2009) 474.
[23] O. Arbouche et al., "First-principles study on structural properties and phase stability of III-phosphide (BP, GaP, AlP and InP)", *Comput. Mater. Sci.*, 47 (2010) 685.
[24] S. Kaur et al., "Emergence of ferromagnetism in vanadium doped aluminium phosphide using density functional theory", *Mater. Today Proc.*, 28 (2020) 1820-1824.
[25] M.Z. Huang and W.Y. Ching, "Calculation of optical excitations in cubic semiconductors. I. Electronic structure and linear response", *Phys. Rev. B*, 47 (1993) 9449.
[26] M. Briki et al., "Relativistic effects on the structural and transport properties of III-V compounds : A first-principles study", *Superlatt. Microstruct.*, 46 (2009) 580-587.
[27] A.H. Reshak and S. Auluck, "Investigation of the electronic properties, first and second harmonic generation for AXIIIBXV zinc-blende semiconductors", *Physica B*, 395 (2007) 143-150.
[28] F. Xie et al., "First-principle study of optical properties of (N,Ga) codoped ZnO", *Opt. Commun.*, 285 (2012) 2660-2664.
[29] Y.F. Tsay, A.J. Corey and S.S. Mitra, "Band structure and optical spectrum of AlP", *Phys. Rev. B*, 12 (1975) 1354-1357.
[30] M. Yousaf et al., "An improved study of electronic band structure and optical parameters of X-phosphides (X=B, Al, Ga, In) by modified Becke-Johnson potential", *Commun. Theor. Phys.*, 58 (2012) 777-784.

Table (1) The lattice constants and bulk modulus for AlP and $Al_{0.75}Sc_{0.25}P$ alloy at different values of pressure (P=0, 5, 10, and 15 GPa)

Materials	a [Å]					B [GPa]			
	P [GPa]	0	5	10	15	0	5	10	15
AlP	Present	5,508	5,407	5,327	5,260	81.424	103.012	122.274	139.755
	Exp	5.47[a]				86[a]			
	Other (0 GPa)	5.511[b], 5.507[b], 5.501[c], 5.451[d], 5.41[h]				82.614[b], 82.5[e], 82.46[f], 83.23[g], 81.1[h]			
$Al_{0.75}Sc_{0.25}P$	Present	5,620	5,511	5,423	5,350	75.210	93.282	111.025	127.692
	Other (0 GPa)								

[a] Ref. [17] [b] Ref. [18] [c] Ref. [19] [d] Ref. [20] [e] Ref. [21] [f] Ref. [22] [g] Ref. [23] [h] [24]

 © ALL RIGHTS RESERVED

Table (2) Direct and indirect band gap of AlP binary compounds and $Al_{0.75}Sc_{0.25}P$ ternary alloy at different pressures (P=0, 5, 10, and 15 GPa)

Materials	$\varepsilon_1(0)$					$\eta(0)$			
	P[GPa]	0	5	10	15	0	5	10	15
AlP	Present	7.58	7.57	7.6	7.64	2.75	2.75	2.76	2.76
	Exp	8[c]				2.75[c]			
	Other (0 GPa)	7.67[a] ; 6.92[b]				2.77[a] ; 2.63[b]			
$Al_{0.75}Sc_{0.25}P$	Present	8.27	8.26	8.38	8.52	2.88	2.87	2.9	2.92

[a] Ref. [29] [b] Ref. [19] [c] Ref. [30]

Table (3) Dielectric constant $\varepsilon_1(0)$ and refractive index n(0) for binary compounds AlP and ternary $Al_{0.75}Sc_{0.25}P$ alloy at different pressures (P=0, 5, 10, and 15 GPa)

Material	Band gap [eV]	P [GPa]			
		0	5	10	15
AlP	E_{G-G}	3.08	3.55	3.94	4.28
	E_{G-X}	1.641	1.524	1.425	1.335
	Exp	2.50[a],2.52[d]			
	Other (E_{G-X})	1.54[b], 1.49[c], 1.594[e]			
$Al_{0.75}Sc_{0.25}P$	E_{G-G}	1.833	1.841	1.839	1.814
	E_{G-X}	2.52	2.59	2.64	2.67

[a] Ref. [25] [b] Ref. [26] [c] Ref. [27] [d] Ref. [1] [e] Ref. [2]

 © ALL RIGHTS RESERVED